

Orbital Nematic Instability in the Two-Orbital Hubbard Model: Renormalization-Group + Constrained RPA Analysis

Masahisa Tsuchiizu,¹ Yusuke Ohno,¹ Seiichiro Onari,² and Hiroshi Kontani¹

¹*Department of Physics, Nagoya University, Nagoya 464-8602, Japan*

²*Department of Applied Physics, Nagoya University, Nagoya 464-8603, Japan*

(Dated: August 1, 2013)

Motivated by the nematic electronic fluid phase in $\text{Sr}_3\text{Ru}_2\text{O}_7$, we develop a combined scheme of the renormalization-group method and the random-phase-approximation-type method, and analyze orbital susceptibilities of the (d_{xz}, d_{yz}) -orbital Hubbard model with high accuracy. It is confirmed that the present model exhibits a ferro-orbital instability near the magnetic or superconducting quantum criticality, due to the Aslamazov-Larkin-type vertex corrections. This mechanism of orbital nematic order presents a natural explanation for the nematic order in $\text{Sr}_3\text{Ru}_2\text{O}_7$, and is expected to be realized in various multiorbital systems, such as Fe-based superconductors.

PACS numbers: 74.70.Pq, 71.10.Fd, 71.27.+a, 75.25.Dk

A bilayer ruthenate compound $\text{Sr}_3\text{Ru}_2\text{O}_7$ has attracted much attention since it exhibits a unique quantum critical behavior [1–4]. Field-induced antiferromagnetic quantum criticality is observed by the many experiments such as the NMR measurements [5]. Surprisingly, the magnetic quantum critical point is hidden by the formation of the nematic electronic liquid phase at very low temperatures ($\sim 1\text{K}$). The orientational-symmetry breaking in the nematic phase is confirmed by the large anisotropy of in-plane resistivity [4, 6, 7]. Thus, the quantum criticality and nematic phase formation are intimately linked in this material [4].

The band structure of the ruthenate oxides are composed of the Ru t_{2g} (d_{xy} , d_{xz} , and d_{yz}) orbitals. For a microscopic understanding of the nematic phase in $\text{Sr}_3\text{Ru}_2\text{O}_7$, a large number of theoretical works have been devoted. The spontaneous violation of the C_4 symmetry of the Fermi surface (FS), i.e., Pomeranchuk instability, had been frequently discussed by focusing on the van Hove singularity. The scenario of the single-band Pomeranchuk instability was originally proposed by using the renormalization-group (RG) method [8], and has been analyzed by the mean-field [9–12] and perturbation [13] studies. However, the temperature-flow (T -flow) RG scheme [14–16] indicates that the nematic fluctuation is always weaker than other instabilities. Thus, the possibility of the single-band Pomeranchuk instability is not settled yet.

An alternative theoretical route to elucidate the nematic phase is to focus on the two d_{xz} and d_{yz} orbitals, which give rise to quasi-one-dimensional α and β bands. It has been pointed out that the nematic state is described as an orbital ordering ($\langle n_{xz} \rangle \neq \langle n_{yz} \rangle$). This ferro-orbital-order scenario has been analyzed within the mean-field-level approximation by focusing only on the $\mathbf{q} = \mathbf{0}$ modes [17–19]. However, the random phase approximation (RPA) leads to the occurrence of the antiferro-orbital order because of the nesting of the FS [20]. Therefore, the theoretical analysis beyond the RPA is required.

Recently, a similar nematic phase in Fe-based superconductors, which are also multiorbital systems, has attracted great attention [21, 22]. Up to now, both the spin nematic [23]

and orbital nematic [24] theories had been proposed. The latter theory pointed out the importance of the vertex correction (VC) in the nematic order. However, they studied a limited number of VCs, so the importance of VCs should be clarified by other unbiased theoretical techniques. For this purpose, the RG treatment is quite suitable because the RG method enables us to perform the systematic calculations of VCs.

In this Letter, we develop an RG scheme and perform accurate evaluations of spin and orbital susceptibilities in the (d_{xz}, d_{yz}) -orbital Hubbard model. We find that the strong orbital nematic fluctuation, i.e., orbital Pomeranchuk instability, emerges near the magnetic or superconducting quantum criticality due to the VCs. The present RG study confirms the validity of our previous perturbation analysis in Ref. [25]. It is confirmed that the two-orbital single-layer Hubbard model is a minimal model to describe the orbital nematic order realized in $\text{Sr}_3\text{Ru}_2\text{O}_7$.

We consider a single-layer (d_{xz}, d_{yz}) -orbital model, where the orbital index $\mu = 1$ and 2 refer to d_{xz} and d_{yz} , respectively. The tight-binding Hamiltonian with tetragonal symmetry is given in the form

$$H_0 = \sum_{\mathbf{k}, \sigma} \sum_{\mu, \mu'=1,2} \xi_{\mathbf{k}}^{\mu\mu'} c_{\mathbf{k}, \mu, \sigma}^\dagger c_{\mathbf{k}, \mu', \sigma}, \quad (1)$$

where $\xi_{\mathbf{k}}^{11} = -2t \cos k_x - 2t_{\text{nn}} \cos k_y + 4t_{\text{nnn}} \cos k_x \cos k_y - \bar{\mu}$, $\xi_{\mathbf{k}}^{22} = -2t \cos k_y - 2t_{\text{nn}} \cos k_x + 4t_{\text{nnn}} \cos k_x \cos k_y - \bar{\mu}$, and $\xi_{\mathbf{k}}^{12} = \xi_{\mathbf{k}}^{21} = 4t' \sin k_x \sin k_y$, with $\bar{\mu}$ the chemical potential. We set $t = 1$ as the energy unit. We also consider the multiorbital Hubbard interactions composed of the intra (inter) orbital interaction U (U'), and the exchange and pair-hopping interaction J . Throughout the Letter, the condition $U = U' + 2J$ is assumed.

The energy band structure and the FSs obtained from H_0 are shown in Fig. 1. The α band forms a holelike FS centered at (π, π) while the β band forms an electronlike FS centered at $(0, 0)$. The RG equations are shown in Fig. 2 (a), where $\chi(\mathbf{q})$, $R(\mathbf{q}; k_1, k_2)$, and $\Gamma(k_1, k_2; k_3, k_4)$ are the susceptibility, the three-point and four-point vertices, respectively [26–29]. The

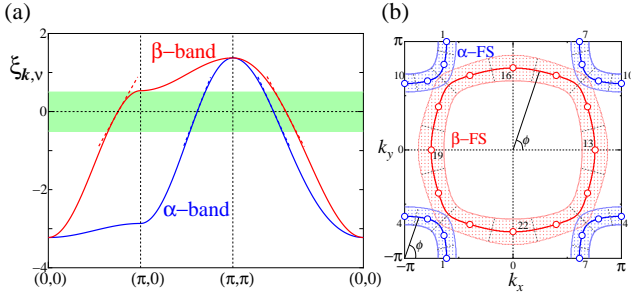


FIG. 1: (color online). (a) Band structure of H_0 for $n = 2.7$. The linearized band dispersions are shown by the dashed lines. The low-energy excitations of electrons ($|\xi_{\mathbf{k},\nu}^{\text{linear}}| \leq \Lambda_0$) are denoted by the shaded area. (b) The patch index (1 – 24) on the FSs.

scattering processes of electrons having energies less than a cutoff Λ_0 are integrated within the RG scheme. In the present analysis we introduce 24 patches shown in Fig. 1 (b). As in previous works, the momenta \mathbf{k}_i in R and Γ are projected onto the Fermi surface, shown in Fig. 1 (b).

In contrast to the conventional patch scheme [16], we take the initial cutoff Λ_0 as a smaller value shown in Fig. 1 (a). Then, we treat the higher-energy contributions ($> \Lambda_0$) by the constrained RPA (cRPA) type method, in which the high-energy interactions are included to the infinite order for RPA-type diagrams. In the present “RG+cRPA scheme”, we calculate the initial values of Γ , R , and χ by the cRPA-type treatment, as shown in Fig. 2. This can be further improved by including the “constrained” VCs perturbatively into the initial values (cRPA+VC method). We will show that the present RG scheme gives small corrections to the initial values, however, provides accurate and nontrivial results for the orbital susceptibilities.

In a conventional patch RG scheme, the higher-energy contributions are treated less accurately because of the projection of momenta on the Fermi surface. In the present scheme, in contrast, the higher-energy contributions can be accurately calculated perturbatively with fine \mathbf{k} meshes. Especially, this treatment is advantageous for the multiorbital model, in which the vertices are \mathbf{k} dependent even in the bare interactions [16]. Thus the present scheme is a natural combination of the merits of the RG (for lower energy) and RPA-type treatment (for higher energy), and enables us to obtain very accurate susceptibilities. This treatment is consistent with the Wick-ordered scheme of the exact functional RG (fRG) formalism in Ref. [16], so the contributions from the RG and cRPA are not overcounted.

In order to analyze the dominant fluctuations in the present two-orbital system, we calculate the susceptibilities by using the RG method. The main purpose of the present Letter is to analyze the quadrupole (orbital) susceptibility at low temperatures. In the present model, there are two irreducible

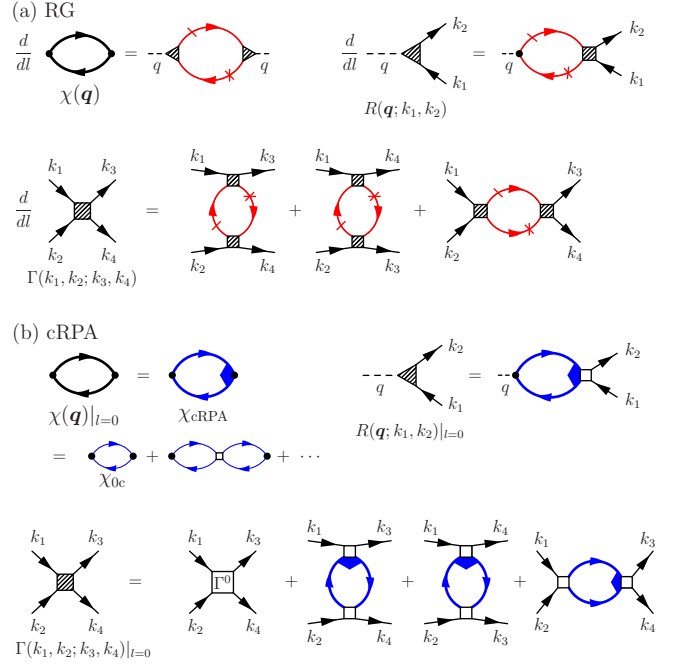


FIG. 2: (color online). The diagrammatic representation of the present RG+cRPA scheme, where l is the scaling parameter. (a) The RG equations for the four-point, three-point vertices, and the susceptibility. The slashed (crossed) line represents an electron propagation having the energy on $\Lambda_{l+dl} < |\xi_{\mathbf{k},\nu}^{\text{linear}}| < \Lambda_l$ ($|\xi_{\mathbf{k},\nu}^{\text{linear}}| < \Lambda_l$), where $\Lambda_l = \Lambda_0 e^{-l}$. (b) The initial values ($l = 0$) of the RG equations are evaluated from the cRPA analysis. The bubbles with thick and thin lines represent $\chi_{\text{cRPA}}(\mathbf{q})$ and $\chi_{0c}(\mathbf{q})$, respectively. The bare four-point vertex represents $\Gamma^0(k_1, k_2; k_3, k_4)$, where $k_i = (\mathbf{k}_i, \nu_i)$.

quadrupole operators [25, 30]:

$$\hat{O}_{x^2-y^2}^j = \sum_{\sigma} (c_{j,1,\sigma}^{\dagger} c_{j,1,\sigma} - c_{j,2,\sigma}^{\dagger} c_{j,2,\sigma}) = n_{j,1} - n_{j,2}, \quad (2)$$

$$\hat{O}_{xy}^j = \sum_{\sigma} (c_{j,1,\sigma}^{\dagger} c_{j,2,\sigma} + c_{j,2,\sigma}^{\dagger} c_{j,1,\sigma}), \quad (3)$$

where j is the site index. The quadrupole susceptibility per spin is given by $\chi_{\gamma}^{\text{q}}(\mathbf{q}) = (1/2) \int_0^{\beta} d\tau (\hat{O}_{\gamma}(\mathbf{q}, \tau) \hat{O}_{\gamma}(-\mathbf{q}, 0))$ ($\gamma = x^2 - y^2$ or xy) where τ is the imaginary time and $\beta = 1/(k_B T)$. The divergence of $\chi_{x^2-y^2}^{\text{q}}(\mathbf{q} = \mathbf{0})$ reflects the emergence of the orbital nematic state ($\langle n_{xz} \rangle \neq \langle n_{yz} \rangle$), which is consistent with the nematic phase in $\text{Sr}_3\text{Ru}_2\text{O}_7$. In addition, we analyze the spin $\chi^{\text{s}}(\mathbf{q})$ and charge $\chi^{\text{c}}(\mathbf{q})$ susceptibilities. In order to confirm the reliability of this treatment, we will show the results in the temperature region where $\chi^{\text{c}}(\mathbf{0})$ remains nonsingular.

In the RPA without VCs [20, 25], $\chi^{\text{sRPA}}(\mathbf{q})$ and $\chi_{x^2-y^2}^{\text{qRPA}}(\mathbf{q})$ are mainly enhanced by U and U' , respectively, and both of them have peak structures at the nesting vector $\mathbf{q} = \mathbf{Q}$ due to the nesting of FSs. $\chi^{\text{sRPA}}(\mathbf{Q})$ is always larger than $\chi_{x^2-y^2}^{\text{qRPA}}(\mathbf{Q})$ for the realistic parameter $U > U'$. We stress that $\chi_{x^2-y^2}^{\text{qRPA}}(\mathbf{q} = \mathbf{0})$ remains small, meaning that the nematic order is not realized in the RPA. Nonetheless, we will show

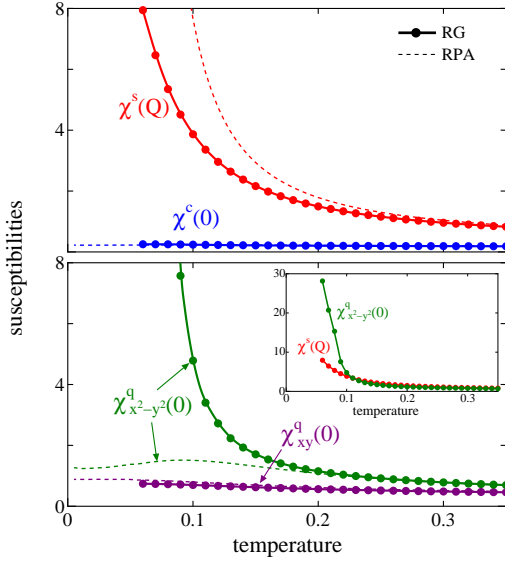


FIG. 3: (color online). Temperature dependences of $\chi^s(\mathbf{Q})$, $\chi^c(\mathbf{0})$ (upper panel), and $\chi_{x^2-y^2}^q(\mathbf{0})$, $\chi_{xy}^q(\mathbf{0})$ (lower panel), for $n = 3.3$, $U = 2.13$, and $U'/U = 0.9$. The solid (dashed) lines represent the RG (RPA) results. In the inset, the same data of $\chi^s(\mathbf{Q})$ and $\chi_{x^2-y^2}^q(\mathbf{0})$ are plotted on a different vertical scale.

that $\chi_{x^2-y^2}^q(\mathbf{0})$ given by the present RG method is strongly enhanced because of the VCs.

In order to analyze low-temperature properties accurately, we linearize the band dispersion within the cutoff scale Λ_0 and change the \mathbf{k} summation into the energy (ξ) integration [31]. In the present numerical study, we consider the case for the electron filling $n = 2.7$ and 3.3 , where we choose the cutoff $\Lambda_0 = 0.5$ and 0.2 , respectively.

First, we focus on the case with large filling $n = 3.3$, where the hopping parameters are chosen as $(t', t_{nn}, t_{nnn}) = (0.1, 0, 0)$. The best nesting vector is given by $\mathbf{Q} \approx (0.35\pi, 0.35\pi)$. Now, we treat the high-energy parts ($> \Lambda_0$) by the cRPA+VC method [32]. The T dependences of the spin, charge, and quadrupole susceptibilities are shown in Fig. 3. By making the direct comparison to the RPA results, we can elucidate the effects of VCs. In the high temperature ($T \gtrsim 0.3$) region, all the susceptibilities exhibit similar behavior to the RPA results [33]. Even at low temperatures, the non-singular susceptibilities $\chi^c(\mathbf{0})$ and $\chi_{xy}^q(\mathbf{0})$ show the same T dependences as in RPA. These facts strongly indicate the reliability of the present RG scheme. The effect of VCs suppresses $\chi^s(\mathbf{Q})$ at low temperatures. The most striking feature of Fig. 3 is the critical enhancement of $\chi_{x^2-y^2}^q(\mathbf{0})$ at low temperatures, which cannot be derived from RPA. In Fig. 4, the momentum dependences of $\chi^s(\mathbf{q})$, $\chi^c(\mathbf{q})$, and $\chi_{x^2-y^2}^q(\mathbf{q})$ for $T = 0.06$ are shown. Since the initial values for $\chi_{x^2-y^2}^q|_{l=0}$ give small contributions and have weak T dependences (inset of Fig. 4), the critical enhancement of $\chi_{x^2-y^2}^q(\mathbf{0})$ is achieved by the RG procedure. We stress that the enhancement in $\chi_{x^2-y^2}^q(\mathbf{q})$ is restricted to the $\mathbf{q} \approx \mathbf{0}$ region, indicating the emergence of the

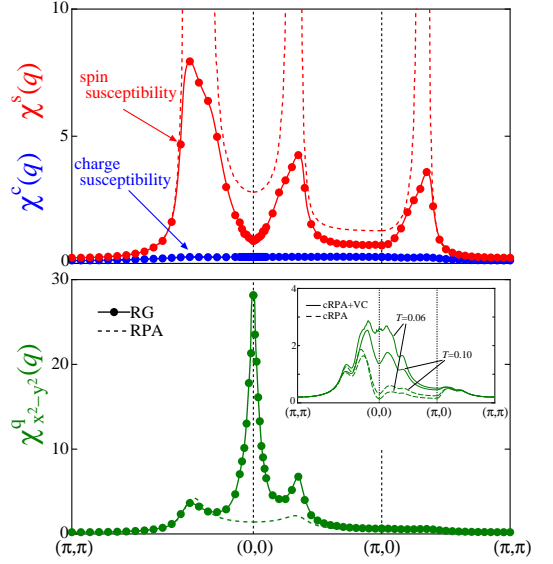


FIG. 4: (color online). Momentum dependences of $\chi^s(\mathbf{q})$, $\chi^c(\mathbf{q})$, and $\chi_{x^2-y^2}^q(\mathbf{q})$ for $T = 0.06$, $n = 3.3$, $U = 2.13$, and $U'/U = 0.9$. The solid (dashed) lines represent the RG (RPA) results. In the inset, the momentum dependences of the initial values for $\chi_{x^2-y^2}^q|_{l=0}$ (solid lines) and the cRPA results (dashed lines) are shown.

orbital nematic order.

Here, we discuss the reason why $\chi_{x^2-y^2}^q(\mathbf{q})$ is critically enhanced only for $\mathbf{q} \approx \mathbf{0}$ in the present RG analysis. The enhancement of the $\mathbf{q} \approx \mathbf{0}$ mode is a strong hallmark of the dominant contributions of the Aslamazov-Larkin (AL) type VCs, since these VCs are known as the enhancement mechanisms of $\mathbf{q} \approx \mathbf{0}$ susceptibilities. In Fig. 3, both $\chi_{x^2-y^2}^q(\mathbf{0})$ and $\chi^s(\mathbf{Q})$ show similar Curie-Weiss behaviors, indicating that the enhancement of $\chi_{x^2-y^2}^q(\mathbf{0})$ originates from the spin fluctuations. As indicated in Refs. [24, 25], the AL term due to the magnetic fluctuations [Fig. 5 (a)] gives the enhancement of $\chi_{x^2-y^2}^q(\mathbf{0})$. Therefore, the magnetic AL term of Fig. 5 (a) is the natural origin of the enhancement of $\chi_{x^2-y^2}^q(\mathbf{0})$. As the origin of the field-induced magnetic quantum criticality, both the van Hove singularity [9–12] and the field-suppression of quantum fluctuation [34] mechanisms had been discussed previously.

Next, we will show the importance of the AL term due to the superconducting fluctuations [Fig. 5 (b)], which was not discussed in Refs. [24, 25]. For this purpose, we introduce the effective interaction for ferro-orbital fluctuations Γ^{quad} and that for superconducting fluctuations Γ^{SCd} , which give the quadrupole and d -wave superconducting susceptibilities: $\Gamma^{\text{quad}} \equiv N_p^{-2} \sum_{p,p'} [2\Gamma(p, p'; p, p') - \Gamma(p, p'; p', p)] \mathcal{O}_p \mathcal{O}_{p'}$ and $\Gamma^{\text{SCd}} \equiv (1/2)N_p^{-2} \sum_{p,p'} \Gamma(p, \bar{p}; p', \bar{p}') \mathcal{D}_p \mathcal{D}_{p'}$, where \mathcal{O}_p is the form factor for $\gamma = x^2 - y^2$ quadrupole: $\mathcal{O}_p = [u_{1\nu}^2(\mathbf{k}(p)) - u_{2\nu}^2(\mathbf{k}(p))] |_{\nu=\nu(p)}$, where $u_{\mu\nu}(\mathbf{k})$ is the unitary matrix for diagonalizing the kinetic term H_0 . Also, \mathcal{D}_p is the d -wave form factor: $\mathcal{D}_p = \cos k_x(p) - \cos k_y(p)$. In the present numerical study, we consider smaller filling

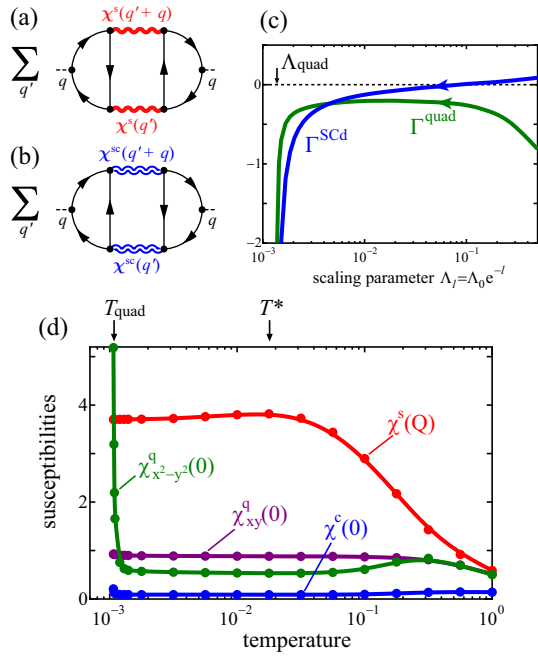


FIG. 5: (color online). (a) The magnetic AL term and (b) the superconducting AL term, where $\chi^{\text{sc}}(\mathbf{q})$ is superconducting propagator. They are proportional to $\sum_{q'} \chi^z(\mathbf{q}') \chi^z(\mathbf{q}' + \mathbf{q})$ ($z = \text{s, sc}$), which takes maximum value at $\mathbf{q} = \mathbf{0}$. (c) The scaling flows of the effective interactions Γ^{quad} and Γ^{SCd} for $n = 2.7$, $U = 2.5$, and $U'/U = 0.98$ at $T = 10^{-10}$. The large negative value of $\Gamma^{\text{quad, SCd}}$ gives the enhancement of the corresponding susceptibility. (d) T dependence of $\chi^{\text{s}}(\mathbf{Q})$, $\chi_{x^2-y^2}^{\text{q}}(\mathbf{0})$, $\chi_{xy}^{\text{q}}(\mathbf{0})$, and $\chi^{\text{c}}(\mathbf{0})$, for $n = 2.7$, $U = 2.5$, and $U'/U = 0.98$.

($n = 2.7$), and put $(t', t_{\text{nn}}, t_{\text{nnn}}) = (0.1, 0.15, 0.03)$ [20], where the best nesting vector is $\mathbf{Q} \approx (0.6\pi, 0.6\pi)$. Here, we employ the cRPA method since the VC for the initial values is not necessary to obtain the orbital nematic fluctuations. The scaling flows of Γ^{quad} and Γ^{SCd} are shown in Fig. 5 (c) [35]. The obtained Γ^{quad} weakly depends on l at high energies, while it exhibits a steep increase in magnitude when $\Lambda_l = \Lambda_{\text{quad}} (\approx 10^{-3})$. This behavior gives the divergent behavior in $\chi_{x^2-y^2}^{\text{q}}(\mathbf{0})$. Moreover, Γ^{SCd} also shows a steep increase in magnitude at $\Lambda_l \approx \Lambda_{\text{quad}}$: This fact means that the development of $\chi_{x^2-y^2}^{\text{q}}(\mathbf{0})$ is closely related to the superconducting fluctuations. From the diagrammatic arguments, we conclude that the major contribution is given by the superconducting AL term in Fig. 5 (b), which represents the coupling between the quadruple and superconducting fluctuations.

The T dependences of the susceptibilities for the case of $n = 2.7$ are shown in Fig. 5 (d) [36]. The spin susceptibility $\chi^{\text{s}}(\mathbf{Q})$ is almost T independent below $T^* \approx 10^{-2}$ due to the effect of nesting deviation. Such a behavior is reminiscent of the Peierls instability in quasi-one-dimensional systems [37, 38]. The quadrupole susceptibility $\chi_{x^2-y^2}^{\text{q}}(\mathbf{0})$ shows a divergent behavior at $T = T_{\text{quad}} \approx 10^{-3}$, which is the same energy scale of the divergent behavior in Γ^{quad} observed in Fig. 5 (c). In contrast, $\chi^{\text{c}}(\mathbf{0})$ and $\chi_{xy}^{\text{q}}(\mathbf{0})$ show no anomaly

even at $T \approx T_{\text{quad}}$, which would ensure the reliability of the singular behavior in $\chi_{x^2-y^2}^{\text{q}}(\mathbf{0})$.

In summary, we have developed the RG+cRPA method for the clarification of the important effects of VCs in susceptibilities, and we have confirmed the orbital Pomeranchuk instability driven by magnetic and superconducting quantum criticalities. In the large-filling case ($n = 3.3$), $\chi_{x^2-y^2}^{\text{q}}(\mathbf{0})$ is critically enhanced by the AL-type VC due to the spin fluctuations, consistently with the predictions in Ref. [25]. In addition, we studied the small-filling case ($n = 2.7$) and also found the development of $\chi_{x^2-y^2}^{\text{q}}(\mathbf{0})$ driven by the superconducting fluctuations. Since the quadrupole operator $\hat{O}_{x^2-y^2}$ represents the order parameter of the orbital ordering [Eq. (2)], both mechanisms would contribute to the nematic phase in $\text{Sr}_3\text{Ru}_2\text{O}_7$. The present mechanisms of the orbital nematic phase would be realized in various multiorbital systems.

The authors are thankful for fruitful discussions with W. Metzner, C. Honerkamp, M. Sigrist, C. Bourbonnais, A.-M.S. Tremblay, H. Yamase, Y. Yamakawa, and D.S. Hirashima. This work was supported by a Grant-in-Aid for Scientific Research from the Ministry of Education, Culture, Sports, Science, and Technology, Japan.

-
- [1] S. A. Grigera, R. S. Perry, A. J. Schofield, M. Chiao, S. R. Julian, G. G. Lonzarich, S. I. Ikeda, Y. Maeno, A. J. Millis, and A. P. Mackenzie, *Science* **294**, 329 (2001).
 - [2] R. Perry, L. Galvin, S. Grigera, L. Capogna, A. Schofield, A. Mackenzie, M. Chiao, S. Julian, S. Ikeda, S. Nakatsuji, et al., *Phys. Rev. Lett.* **86**, 2661 (2001).
 - [3] S. A. Grigera, R. A. Borzi, A. P. Mackenzie, S. R. Julian, R. S. Perry, and Y. Maeno, *Phys. Rev. B* **67**, 214427 (2003).
 - [4] A. P. Mackenzie, J. A. N. Bruin, R. A. Borzi, A. W. Rost, and S. A. Grigera, *Physica C* **481**, 207 (2012), and references therein.
 - [5] K. Kitagawa, K. Ishida, R. S. Perry, T. Tayama, T. Sakakibara, and Y. Maeno, *Phys. Rev. Lett.* **95**, 127001 (2005).
 - [6] S. A. Grigera, P. Gegenwart, R. A. Borzi, F. Weickert, A. J. Schofield, R. S. Perry, T. Tayama, T. Sakakibara, Y. Maeno, A. G. Green, et al., *Science* **306**, 1154 (2004).
 - [7] R. A. Borzi, S. A. Grigera, J. Farrell, R. S. Perry, S. J. S. Lister, S. L. Lee, D. A. Tennant, Y. Maeno, and A. P. Mackenzie, *Science* **315**, 214 (2007).
 - [8] C. J. Halboth and W. Metzner, *Phys. Rev. Lett.* **85**, 5162 (2000).
 - [9] H. Yamase and A. A. Katanin, *J. Phys. Soc. Jpn.* **76**, 073706 (2007).
 - [10] H. Yamase, *Phys. Rev. B* **80**, 115102 (2009).
 - [11] M. H. Fischer and M. Sigrist, *Phys. Rev. B* **81**, 064435 (2010).
 - [12] H. Yamase and P. Jakubczyk, *Phys. Rev. B* **82**, 155119 (2010).
 - [13] Y. Yoshioka and K. Miyake, *J. Phys. Soc. Jpn.* **81**, 023707 (2012).
 - [14] C. Honerkamp and M. Salmhofer, *Phys. Rev. B* **64**, 184516 (2001).
 - [15] C. Honerkamp, *Phys. Rev. B* **72**, 115103 (2005).
 - [16] W. Metzner, M. Salmhofer, C. Honerkamp, V. Meden, and K. Schönhammer, *Rev. Mod. Phys.* **84**, 299 (2012).
 - [17] S. Raghu, A. Paramakanti, E. A. Kim, R. A. Borzi, S. A. Grigera, A. P. Mackenzie, and S. A. Kivelson, *Phys. Rev. B* **79**,

- 214402 (2009).
- [18] W.-C. Lee and C. Wu, Phys. Rev. B **80**, 104438 (2009).
- [19] K. W. Lo, W.-C. Lee, and P. W. Phillips, Europhys. Lett. **101**, 50007 (2013).
- [20] T. Takimoto, Phys. Rev. B **62**, 14641 (2000).
- [21] J.-H. Chu, J. G. Analytis, K. De Greve, P. L. McMahon, Z. Islam, Y. Yamamoto, and I. R. Fisher, Science **329**, 824 (2010).
- [22] M. Yoshizawa, D. Kimura, T. Chiba, S. Simayi, Y. Nakanishi, K. Kihou, C.-H. Lee, A. Iyo, H. Eisaki, M. Nakajima, et al., J. Phys. Soc. Jpn. **81**, 024604 (2012), and references therein.
- [23] R. M. Fernandes, L. H. VanBebber, S. Bhattacharya, P. Chandra, V. Keppens, D. Mandrus, M. A. McGuire, B. C. Sales, A. S. Sefat, and J. Schmalian, Phys. Rev. Lett. **105**, 157003 (2010).
- [24] S. Onari and H. Kontani, Phys. Rev. Lett. **109**, 137001 (2012).
- [25] Y. Ohno, M. Tsuchiizu, S. Onari, and H. Kontani, J. Phys. Soc. Jpn. **82**, 013707 (2013).
- [26] C. Bourbonnais, B. Guay, and R. Wortis, *Theoretical Methods for Strongly Correlated Electrons* (Springer, New York, 2003), p. 77.
- [27] D. Zanchi and H. J. Schulz, Europhys. Lett. **44**, 235 (1998).
- [28] D. Zanchi and H. J. Schulz, Phys. Rev. B **61**, 13609 (2000).
- [29] C. J. Halboth and W. Metzner, Phys. Rev. B **61**, 7364 (2000).
- [30] H. Kontani, T. Saito, and S. Onari, Phys. Rev. B **84**, 024528 (2011).
- [31] T. Nishine, M. Tsuchiizu, and Y. Suzumura, J. Phys.: Conf. Ser. **132**, 012020 (2008).
- [32] In the present calculations of Figs. 3 and 4, we improved the cRPA method by including the VC due to higher-energy contributions, since the initial value for the the nematic instability is underestimated due to the artifact of the the cRPA treatment. The obtained initial values for the quadrupole susceptibilities are shown in the inset of Fig. 4. The small and nonsingular contributions of the constrained VCs at $\mathbf{q} \approx \mathbf{0}$ is enough to produce the strong development of $\chi_{x^2-y^2}^q(\mathbf{0})$ by RG. See Supplemental Material at <http://link.aps.org/supplemental/10.1103/PhysRevLett.111.057003> for details on the cRPA+VC method.
- [33] J. E. Hirsch, Phys. Rev. B **31**, 4403 (1985).
- [34] K. Sakurazawa, H. Kontani, and T. Saso, J. Phys. Soc. Jpn. **74**, 271 (2005).
- [35] We have verified that the similar scaling behavior of Γ^{quad} to Fig. 5 (c) is obtained by the T -flow RG scheme [14].
- [36] In usual one-loop RG analyses, the coupling Γ_l could diverge before the convergence of the l integration in $\chi^z(\mathbf{0})$ is achieved [14]. To overcome this difficulty, in calculating Fig. 5 (d), we stop the renormalization of Γ if one of them reaches to 10^3 in magnitude.
- [37] R. Duprat and C. Bourbonnais, Eur. Phys. J. B **21**, 219 (2001).
- [38] H. Nelisse, C. Bourbonnais, H. Touchette, Y. M. Vilc, and A.-M. S. Tremblay, Eur. Phys. J. B **12**, 351 (1999).

Supplemental Material

Initial function due to cRPA+VC method

Masahisa Tsuchiizu,¹ Yusuke Ohno,¹ Seiichiro Onari,² and Hiroshi Kontani¹

¹*Department of Physics, Nagoya University, Nagoya 464-8602, Japan*

²*Department of Applied Physics, Nagoya University, Nagoya 464-8603, Japan*

In the present RG method, we introduce the cutoff energy Λ_0 according to the functional RG theory [1]. We set Λ_0 so as that the topology of the constant energy surfaces $\xi_{\mathbf{k},\nu} = \varepsilon$ ($\xi_{\mathbf{k},\nu}$ being the ν -th band dispersion) for $|\varepsilon| < \Lambda_0$ is equivalent to the Fermi surface. In the present work, the scattering processes under the cutoff Λ_0 are calculated by solving the one-loop RG equations, by dividing the Fermi surfaces into N_p patches. The four-point vertex with higher-energy contributions, $\hat{\Gamma}^H(\mathbf{p}\sigma, \mathbf{p}'\sigma'; \mathbf{k}\rho, \mathbf{k}'\rho')$, is incorporated as the initial values of the RG differential equations, where \mathbf{k} and \mathbf{p} (σ and ρ) are momentum (spin) indices. According to the functional RG theory [1], $\hat{\Gamma}^H$ is constructed by the Coulomb interaction (U, U', J) in addition to the higher and lower energy Green functions, $G_\nu^H(\mathbf{k}) \equiv G_\nu(\mathbf{k}) \Theta(|\xi_{\mathbf{k},\nu}| - \Lambda_0)$ and $G_\nu^L(\mathbf{k}) \equiv G_\nu(\mathbf{k}) \Theta(\Lambda_0 - |\xi_{\mathbf{k},\nu}|)$ respectively, under the constraint that $\hat{\Gamma}^H$ is irreducible with respect to the product of G_ν^L .

By virtue of introducing the cutoff energy Λ_0 , we can perform the RG calculation with high accuracy since the topology of the constrained energy surfaces is unchanged in the lower energy regime. We also calculate the higher-energy contributions by using the perturbative methods. In the present study, we apply (i) the constrained RPA (cRPA) method, and also apply (ii) the cRPA method with higher-order vertex corrections.

Hereafter, we derive the expression of Γ^H on the d -orbital basis, which should be converted to the patch index to use as the initial values of the RG equations. The spin and charge susceptibilities in the cRPA are given by the following ($N_{\text{orb}}^2 \times N_{\text{orb}}^2$) matrix form (N_{orb} is the number of orbital degrees of freedom):

$$\hat{\chi}_{\text{cRPA}}^{\text{s(c)}}(q) = \frac{\hat{\chi}_{0\text{c}}(q)}{1 - \hat{\Gamma}^{\text{s(c)}} \hat{\chi}_{0\text{c}}(q)}, \quad (1)$$

where $\hat{\Gamma}^{\text{s(c)}}$ is the bare interaction for the spin (charge) channel given in Ref. 2, and $q = (\mathbf{q}, 2\pi lT)$. The constrained bare susceptibility $\hat{\chi}_{0\text{c}}(\mathbf{q})$ is given by

$$\begin{aligned} [\hat{\chi}_{0\text{c}}(q)]_{l,l',m,m'} &= -T \sum_{\mathbf{k}} G_{l,m}(\mathbf{k} + q) G_{m',l'}(\mathbf{k}) \\ &+ T \sum_{\mathbf{k}} G_{l,m}^L(\mathbf{k} + q) G_{m',l'}^L(\mathbf{k}), \quad (2) \end{aligned}$$

where l, l', m, m' are the orbital indices, $k = (\mathbf{k}, \pi(2n + 1))$

$\pi T)$, and $G_{l,m}^L(\mathbf{k})$ is the Green function on the orbital basis given by the unitary transformation from $G_\nu^L(\mathbf{k})$.

In method (i), we approximate $\Gamma_{l,l',m,m'}^H(\mathbf{p}\sigma, \mathbf{p}'\sigma'; \mathbf{k}\rho, \mathbf{k}'\rho')$ in the ($N_{\text{orb}}^2 \times N_{\text{orb}}^2$) matrix form as

$$\begin{aligned} \hat{\Gamma}^H(\mathbf{p}\sigma, \mathbf{p}'\sigma'; \mathbf{k}\rho, \mathbf{k}'\rho') &= \hat{\Gamma}_{\sigma,\sigma';\rho,\rho'}^0 \\ &+ \hat{V}_{\sigma,\sigma';\rho,\rho'}(\mathbf{p} - \mathbf{p}') - \hat{V}'_{\sigma,\sigma';\rho,\rho'}(\mathbf{p} - \mathbf{k}), \quad (3) \end{aligned}$$

where $\hat{\Gamma}^0$ is the antisymmetrized bare Coulomb interaction with spin indices ($\sigma, \sigma', \rho, \rho'$). Considering the SU(2) symmetry of the spin space, it is expressed as

$$\hat{\Gamma}_{\sigma,\sigma';\rho,\rho'}^0 \equiv \hat{\Gamma}^c \delta_{\sigma,\sigma'} \delta_{\rho',\rho} + \hat{\Gamma}^s \boldsymbol{\sigma}_{\sigma,\sigma'} \cdot \boldsymbol{\sigma}_{\rho',\rho}, \quad (4)$$

where $\boldsymbol{\sigma}$ is the Pauli matrix vector. Also, \hat{V} is given as

$$\hat{V}_{\sigma,\sigma';\rho,\rho'}(\mathbf{q}) = \hat{V}^c(\mathbf{q}, 0) \delta_{\sigma,\sigma'} \delta_{\rho',\rho} + \hat{V}^s(\mathbf{q}, 0) \boldsymbol{\sigma}_{\sigma,\sigma'} \cdot \boldsymbol{\sigma}_{\rho',\rho}, \quad (5)$$

where $\hat{V}^{\text{s(c)}}(q) = \hat{\Gamma}^{\text{s(c)}} \hat{\chi}_{\text{cRPA}}^{\text{s(c)}}(q) \hat{\Gamma}^{\text{s(c)}}$. In addition, $[\hat{V}'_{\sigma,\sigma';\rho,\rho'}(\mathbf{q})]_{l,l',m,m'} \equiv [\hat{V}_{\sigma,\sigma';\rho,\rho'}(\mathbf{q})]_{l,m;l',m'}$.

In method (i), the initial value in Eq. (3) is underestimated for $\mathbf{p} = \mathbf{p}'$ and $\mathbf{k} = \mathbf{k}'$ because of the reason $\hat{\chi}_{\text{cRPA}}^{\text{s(c)}}(\mathbf{0}, 0) \approx 0$ for $T \ll \Lambda_0$. This relation in the cRPA is unfavorable for the development of the susceptibilities at $\mathbf{q} = \mathbf{0}$, by solving the RG equations. However, this relation is an artifact of the cRPA, and it will not be satisfied in general. In method (ii), therefore, we improve the initial value Γ^H in Eq. (3), by introducing the vertex correction into the cRPA as

$$\hat{\chi}_{\text{cRPA+VC}}^{\text{s(c)}}(q) = \frac{\hat{\chi}_{0\text{c}}(q) + \hat{X}^{\text{s(c)}}(q)}{1 - \hat{\Gamma}^{\text{s(c)}} [\hat{\chi}_{0\text{c}}(q) + \hat{X}^{\text{s(c)}}(q)]}, \quad (6)$$

where $\hat{X}^{\text{s(c)}}(q)$ is the vertex correction (VC) due to higher-energy contribution. Then, the initial function is improved by replacing $\hat{\chi}_{\text{cRPA}}(q)$ with $\hat{\chi}_{\text{cRPA+VC}}(q)$ in Eq. (3). Here, we calculate the VC up to the second-order diagrams with respect to $\hat{\chi}_{\text{cRPA}}(q)$: The first-order term is called the Maki-Thompson (MT) term, and the second-order term is called the Aslamazov-Larkin (AL) term [2]. We find that the MT term is negligibly small, and only the AL term for the charge channel is quantitatively important. It is given by

$$X_{l,l',m,m'}^c(q) = \frac{T}{2} \sum_k \sum_{a \sim h} \Lambda_{ll',ab,ef}(q; k) \left[V_{ab,cd}^c(k+q) V_{ef,gh}^c(-k) + 3V_{ab,cd}^s(k+q) V_{ef,gh}^s(-k) \right] \Lambda'_{mm',cd,gh}(q; k). \quad (7)$$

Here, $\hat{\Lambda}(q; k)$ is the three-point vertex due to higher-energy contribution, given as

$$\Lambda_{mm',cd,gh}(q; k) = \sum_{A,B,C} T \sum_p G_{m,c}^A(p+q) G_{d,g}^B(p-k) G_{h,m'}^C(p), \quad (8)$$

where $p = (\mathbf{p}, \pi(2n' + 1)T)$, and $\Lambda'_{mm',cd,gh}(q; k) \equiv \Lambda_{ch,mg,dm'}(q; k) + \Lambda_{gd,mc,hm'}(q; -k - q)$. The summations with respect to A, B, C are taken as $(A, B, C) = (\text{H}, \text{H}, \text{H}), (\text{L}, \text{H}, \text{H}), (\text{H}, \text{L}, \text{H}), (\text{H}, \text{H}, \text{L})$. Here, $\hat{X}^c(q)$ is irreducible with respect to the product of $G_{l,m}^L(k)$.

Within the cRPA, the initial interaction $V(\mathbf{q})$ in Eq. (5) is small for the forward scattering ($\mathbf{q} = \mathbf{0}$) at low temperatures since $\chi_{0c}(\mathbf{q}, \omega = 0)|_{\mathbf{q}=\mathbf{0}} = \sum_{\mathbf{k}} (-df/d\epsilon)_{\epsilon=\xi_{\mathbf{k}}} \theta(|\xi_{\mathbf{k}}| - \Lambda) \approx 0$ at $T \ll \Lambda$. However, the VC $X(\mathbf{q})$ in Eq. (7) is finite at $T \ll \Lambda$, since the constrained three-point vertex in Eq. (8) is finite even for $\mathbf{q} \approx \mathbf{0}$, which can be proved analytically as well as numerically. Therefore, the VC gives a finite contribution to $\hat{\chi}_{\text{cRPA+VC}}^c(\mathbf{0})$, as seen in Eq. (6), and the smallness of $\hat{\chi}_{\text{cRPA}}^c(\mathbf{0})$ is an artifact of the cRPA due to the absence of the VC.

Diagrammatically, $\hat{X}^{s(c)}(q)$ is the second-order term with respect to $\hat{\chi}_{\text{cRPA}}(q)$ composed of multiple $G = (G^{\text{H}}, G^{\text{L}})$: The latter constructs the three-point vertex in Eq. (8). In calculating Eq. (8), we introduce another cutoff energy $\Lambda_1 (> \Lambda_0)$ and put $G_{\nu}(k) = 0$ for $|\xi_{\mathbf{k},\nu}| > \Lambda_1$ in the band-diagonal basis: Although the VC is underestimated by introducing Λ_1 , we can drop the almost momentum-independent contribution to the VC, which is unimportant for the RG result. In the present

study, we put $\Lambda_1 = 0.6 (= 3\Lambda_0)$: the obtained $\hat{X}^{s(c)}(q)$ is very similar for $\Lambda_1 = 0.4 \sim 1.0$.

In the present method, the contributions from the RG and the constrained perturbation are not overcounted, since $\hat{\Gamma}^{\text{H}}$ in this study is constructed consistently with the Wick-ordered scheme of the exact functional RG formalism [1]. In addition, $\hat{X}^{s(c)}(\mathbf{q}) \ll \hat{\chi}_{0c}(\mathbf{q})$ except for $q_{\mu} \approx 0$ ($\mu = x, y$), and the smallness of $\hat{\chi}_{0c}(\mathbf{q})$ at $q_{\mu} \approx 0$ is an artifact of the approximation, as shown in Fig. 4 (b) in the main text. This fact means that the perturbative treatment with respect to $\hat{\chi}_{\text{cRPA}}(\mathbf{q})$ given by the present study is justified. The large nematic susceptibility given by the present work originates from the development of the low-energy four-point vertex given by the RG equations. By virtue of the present RG+cRPA type approximation, we obtain beautiful temperature- and momentum-dependences of the susceptibilities numerically.

-
- [1] W. Metzner, M. Salmhofer, C. Honerkamp, V. Meden, and K. Schönhammer, *Rev. Mod. Phys.* **84**, 299 (2012).
 [2] S. Onari and H. Kontani, *Phys. Rev. Lett.* **109**, 137001 (2012).